

Co and Fe doped SnO₂ nanorods by Ce co-doping and their electrical and magnetic properties

Jasneet Kaur^{1*}, Jaspreet Kaur¹, R.K. Kotnala², Vinay Gupta³, Kuldeep Chand Verma¹

¹Department of Physics, Eternal University, Baru Sahib, Sirmour (H.P.) 173101, India

²National Physical Laboratory, New Delhi 110012, India

³Department of Physics and Astrophysics, University of Delhi, Delhi 110007, India

*Corresponding author. Tel: (+91) 9882711636; E-mail: jasneet.physics@gmail.com

ABSTRACT

In the present work, the self-assembly of Co²⁺ and Fe³⁺ doped SnO₂ nanoparticles (Co and Fe = 5 mol% each) into nanorods by co-doping of Ce³⁺ (4 mol%) ions is studied. The nanorods are prepared by a chemical route using polyvinyl alcohol as surfactant with the composition Sn_{0.91}Co_{0.05}Ce_{0.04}O₂ (SCC54) and Sn_{0.91}Fe_{0.05}Ce_{0.04}O₂ (SFC54). The X-ray diffraction (XRD), transmission electron microscopy (TEM), magnetic and electrical measurements are used to characterize these nanorods. The XRD pattern show the tetragonal rutile and polycrystalline nature of SnO₂ nanorods which is also confirmed by TEM. The TEM images exhibit that the diameter of SCC54 nanorods lie in the range of 15-20 nm, length~100-200 nm whereas for SFC54 specimen, diameter ~5-15 nm and length ~50-100 nm. In our previous work, we fabricated Co and Fe (3 and 5 mol% each) doped SnO₂ nanoparticles which exhibited high ferromagnetism. It is observed that on Ce³⁺ co-doping, nanoparticles assembled themselves into rod like structures and the values of saturation magnetization and dielectric properties have further enhanced. Thus the nature and the concentration of dopants are found to play crucial role in tuning the morphology, magnetic and electrical properties of nanostructures. The values of saturated magnetization (*M_s*) are 1.14 and 0.14 emu/g and coercive field are 112 and 42 Oe, in SCC54 and SFC54 specimen, respectively, at room temperature. The variation in dielectric behavior is attributed due to the interface polarization. However, in lower frequency regime, the decreasing trend of dielectric permittivity with increasing frequency is explained by the Maxwell-Wagner theory and Koops' model, whereas, in higher frequency region, the resonant behavior is observed due to nano size effect. Copyright © 2012 VBRI Press.

Keywords: Nanorods; sol-gel; TEM; magnetic properties; dielectric behavior.



Jasneet Kaur is a research scholar in the Department of Physics, Eternal University, Baru Sahib, India. She did her B.Sc. Physics (Honors) and M.Sc. Physics from University of Delhi, Delhi, India. Her main research interests are synthesis and structural, electrical, magnetic and optical characterization of dilute magnetic semiconductor (DMS) SnO₂ based nanostructures.

Introduction

Ferromagnetism of diluted magnetic semiconductors (DMSs) produced is significantly increased due to their potential technological applications in the field of spintronics, nanoelectronics, nanophotonics, magnetoelectronics, and microwave devices [1-4]. In search of these type of materials with high ferromagnetic Curie temperatures along with precise controllable spin

properties, wide band gap oxide based DMSs such as TiO₂, ZnO, SnO₂, and HfO₂ doped with transition metal (TM) ions (Co, Mn, Ni, Fe, Cr, etc.) have attracted considerable attention resulting from large sp-d exchange interaction between the magnetic ions and the band electrons.

Among these oxides, SnO₂ is an important n-type semiconductor with wide energy gap material (*E_g* = 3.62 eV at 300 K) and presents special properties, such as transparency or remarkable chemical and thermal stabilities, with direct applications for photodetectors, catalysts for oxidation and hydrogenation, solar cells, semiconducting gas sensors, liquid crystal displays, protective coatings, etc. [5]. Many works reported ferromagnetic properties of TM-doped SnO₂ thin films and nanoparticles. Ogale *et al.* [6] reported room-temperature ferromagnetism in pulsed laser deposited SnO₂: Co (5 and 27%) thin films. More recently, Fitzgerald *et al.* [7] found ferromagnetism in Co-doped SnO₂ thin films for Co contents ranging from 0.1 to 15%. On the other hand ferromagnetism in Sn_{0.95}Fe_{0.05}O₂ ceramic with magnetic moment of 0.95 μB/Fe, about 85% of the iron being in a

magnetically ordered high-spin Fe^{3+} and Curie temperature of about 360 K were reported by Fitzgerald *et al.* [8] On the other hand, Punnoose *et al.* [9] reported a paramagnetic behavior in chemically synthesized powder sample $\text{Sn}_{0.95}\text{Fe}_{0.05}\text{O}_2$ prepared above 600°C and Adhikari *et al.* [10] observed an antiferromagnetic behavior of 5% Fe-doped SnO_2 nanoparticles synthesized by a chemical co-precipitation method. Overall, the origin of ferromagnetism in TM doped SnO_2 system is controversial and more detailed investigations are required.

Nano metric size has great influence on the performance of several material systems and may affect various physical properties not only the host semiconductors but also of the DMS materials derived from them. For example, when the crystallite size of some of the DMS materials is reduced to below 30 nm, they are found to exhibit better ferromagnetic properties when compared with those having microcrystalline particles (>100 nm). Apart from this, nanocrystalline oxide DMS materials may be exploited for a variety of applications such as spintronics devices, biomedical applications, magnetic storage devices, ferrofluids, etc. Therefore, it is important to study the influence of nano metric size on various physical properties of oxide based diluted magnetic semiconductors. Among the oxide based DMS materials, SnO_2 exhibits remarkable behavior because of native oxygen vacancies, high carrier density and transparency, and high chemical and thermal stabilities.

A few studies [5,8,10] on nanocrystalline Co and Fe-doped SnO_2 powders with conflicting results especially on the existence of room temperature ferromagnetism were reported. In view of this, it is clear that applying appropriate growth conditions would be a crucial factor in order to obtain the room temperature ferromagnetism. Moreover, many research works have been reported on dielectric properties of transition metal doped SnO_2 nanostructures. The conduction mechanism in SnO_2 has been thoroughly studied by Ogawa *et al.* [11] using Hall measurements. Several methods used by researchers to prepare SnO_2 DMS are chemical co-precipitation, conventional mixed oxide, sol-gel, hydrothermal processing etc [12]. Therefore, effort has been made by the authors in the present investigation to test whether the room temperature ferromagnetism is possible with

Co and Fe-doped and Ce co-doped SnO_2 nanorods. Moreover, the structural, microstructural and electrical properties and the co-doping of Ce^{3+} ions in the fabrication of nanorods have also been studied.

Experimental

SCC54 and SFC54 nanorods were prepared by a chemical route using PVA as surfactant. The precursor solutions were prepared from stannic chloride pentahydrate ($\text{SnCl}_4 \cdot 5\text{H}_2\text{O}$), ferric chloride (FeCl_3), cobalt chloride ($\text{CoCl}_2 \cdot 6\text{H}_2\text{O}$) and cerium chloride ($\text{CeCl}_3 \cdot 7\text{H}_2\text{O}$). The detailed experimental procedure is presented elsewhere [13]. The crystalline structure was analyzed by X-ray diffraction (XRD) using X-Pert PRO system and microstructure by transmission electron microscopes (TEM) of Hitachi H-7500. The magnetic measurements

were performed at room temperature using a vibrating sample magnetometer (VSM-735), and the electrical measurements were performed at room temperature using an impedance analyzer (4200 semiconductor character unit, CVU module). For electrical measurements, the annealed powder was pressed into pellets of thickness ~ 0.5 mm by cold isotatic pressing method with a pressure of 5 bar for 5 min and then sintered.

Results and discussion

Fig. 1 shows the XRD patterns of SCC54 and SFC54 nanorods annealed at 700 °C/2h. All the diffraction peaks can be well indexed to the tetragonal rutile structure of parent SnO_2 , which belong to the space group of $\text{P4}_2/\text{mmm}$ and shows that on doping with Co, Fe and co-doping with Ce, a similar pattern is observed, without any extra diffraction peaks from Co, Fe, Ce or other impurities.

The surface morphology by TEM images of SCC54 and SFC54 nanorods is illustrated in **Fig. 2**. It shows the crystalline and nano behavior of each specimen. The diameter of the SCC54 nanorods lies in the range of 15-20 nm and length of 150-200 nm whereas SFC54 consist of two morphologies, nanospheres and nanorods (average grains size 11 nm); nanorods of diameter is 5-15 nm and length 50-100 nm. A proposed growth mechanism of cerium co-doped SnO_2 nanorods can be explained in terms of chemical reactions and crystal growth. From the crystallization point of view, the synthesis of an oxide during an aqueous solution reaction is expected to experience nucleation-growth process [5].

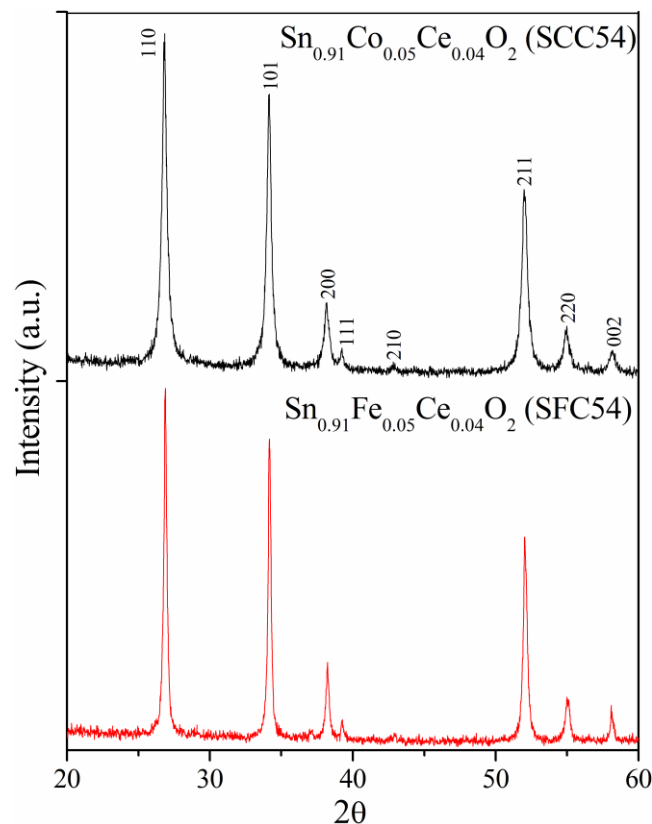


Fig 1. XRD pattern SCC54 and SFC54 nanorods.

Fig. 3 shows the room temperature ferromagnetism of both SCC54 and SFC54 specimens. The values of saturated magnetization (M_s) are 1.14 and 0.14 emu/g and coercive field are 112 and 42 Oe, respectively, observed in SCC54 and SFC54 specimens. The inset of **Fig. 3** shows the variation of dielectric constant (ϵ) and loss ($\tan\delta$) with frequency at room temperature. The ϵ decreases rapidly in lower frequency regime because of space charge contribution. However, in frequency range from 100 kHz - 7 MHz in SCC54 and from 100 kHz - 9 MHz in SFC54, shows dispersionless dielectric response. A rapid change in ϵ at higher frequency occurs due to resonance effect. At 1MHz, the values of ϵ are 39 and 28, respectively, for SCC54 and SFC54 specimens.

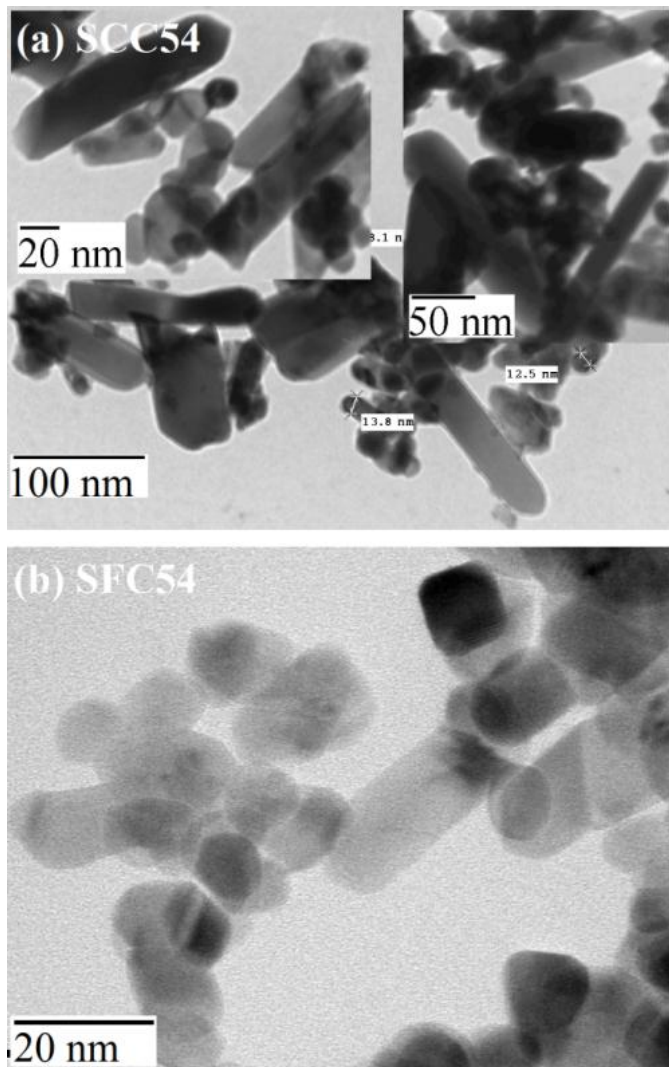


Fig. 2. TEM images.

As shown in **Fig. 3**, the observed dielectric behaviour is frequency dependent which can also be explained on the basis of Maxwell-Wagner model [3]. According to this model, a dielectric medium is assumed to be made of well conducting grains which are separated by poorly conducting (or resistive) grain boundaries. Under the application of external electric field, the charge carriers can easily migrate into the grains but are accumulated on the grain boundaries. This process can produce large polarization and high

dielectric constant. The small conductivity of grain boundary contributes to the high value of dielectric constant at low frequency. The higher value of dielectric constant can also be explained on the basis of interfacial/space charge polarization due to inhomogeneous dielectric structure. The inhomogeneity present in the system may be due to porosity or grain structure. The polarization decreases with the increase in frequency and then reaches a constant value which is due to the fact that beyond a certain frequency of external field the hopping between different metal ions (Sn^{4+} , Co^{2+} or Fe^{3+} and Ce^{3+}) cannot follow the alternating field. It has also been observed that the value of dielectric constant has been increased with the incorporation of dopants [13]. It may be due to the high dielectric polarizability of cobalt and iron ions and very high polarizability of cerium ions as compared to tin. Hence, as the dopant concentration increases more tin ions will be substituted by the dopant ions and thereby, increasing the dielectric polarization, which in turn increases the dielectric constant.

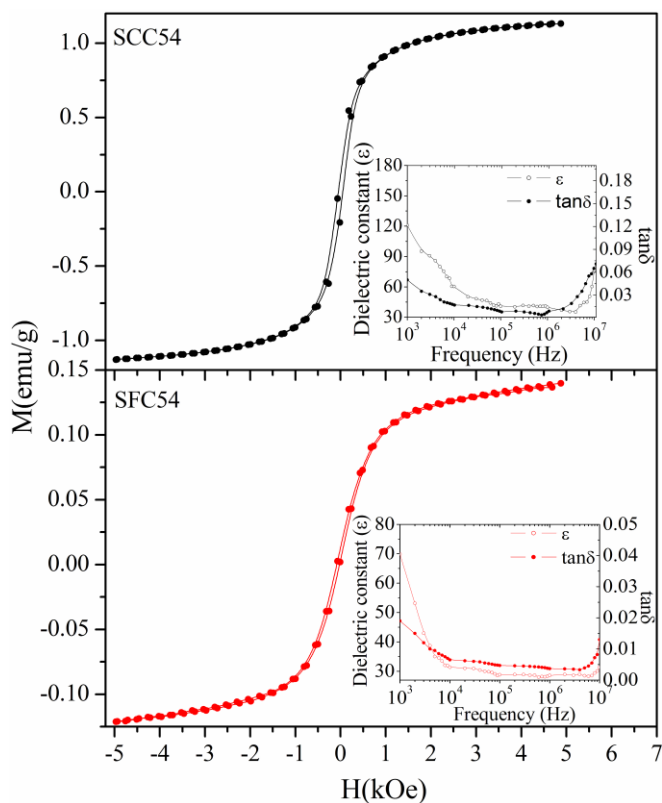


Fig. 3. M - H hysteresis and inset shows dielectric constant and loss variation with frequency.

Loss tangent or loss factor ($\tan\delta$) represents the energy dissipation in the dielectric system. The loss factor of SCC54 and SFC54 nanostructures decreases in the frequency range up to 10 kHz (**Fig. 3** inset) and it increases at the frequencies above 10 kHz, and reaches the maximum values at a frequency of 10 MHz. According to Koops' model [4], the decrease of the $\tan\delta$ is explained by the fact that at lower frequencies, where the resistivity is high and the grain boundary effect is dominant, thus more energy is required for the exchange of electrons between the metal ions and dopant ions located at grain boundaries, i.e. energy

loss ($\tan\delta$) is high whereas, at high frequencies, the resistivity is comparatively lower and grains themselves play a dominant role, thus very small amount of energy is required for hopping of electrons between the ions located in a grain, and therefore, $\tan\delta$ is also small. The maximum value of the tangent of losses is observed when hopping frequency corresponds to the frequency of the external field.

Conclusion

SCC54 and SFC54 nanorods are prepared successfully by Ce co-doping in $\text{Sn}_{0.95}\text{Co}_{0.05}\text{O}_2$ and $\text{Sn}_{0.95}\text{Fe}_{0.05}\text{O}_2$ composition by sol gel method. XRD patterns show the tetragonal rutile phase of these nanorods. The TEM measurements exhibit that the diameter of SCC54 nanorods lies in the range of 15-20 nm and length of 150-200 nm and SFC54 nanorods of diameter is 5-15 nm and length 50-100 nm. Maxwell-Wagner theory and space charge polarization are used to explain the frequency dependent dielectric constant. The tangent loss is explained by the Koops' model. The values of M_s are 1.14 and 0.14 emu/g and coercive field are 112 and 42 Oe, for SCC54 and SFC54 specimens respectively.

Reference

1. Kaur, J.; Shah, J.; Kotnala, R.K.; Verma, K.C. *Ceramics international* **2012**, 38, 5563.
2. Daniel, V.V. *Dielectric Relaxation*. Academic Press, London, **1967**.
3. Wagner, K.W. *Am. J. Phys.* **1973**, 40, 317.
4. Koops, C.G. *Phys. Rev.* **1951**, 83, 121.
5. Punnoose, A.; Reddy K.M.; Hays J.; Thurber A.; Engelhard M.H. *Appl. Phys. Lett.* **2006**, 89, 112509.
6. Ogale, S.B.; Choudhary, R.J.; Buban, J.P.; Lofland, S.E.; Shinde, S.R.; Kale, S.N.; Kulkarni, V.N.; Higgins, J.; Lanci, C.; Simpson, J.R.; Browning, N.D.; Sharma, S.D.; Drew, H.D.; Greene, R.L.; Venkatesan, T. *Phys. Rev. Lett.* **2003**, 91, 077205.
7. Fitzgerald, C.B.; Venkatesan, M.; Dorneles, L.S.; Gunning, R.; Stamenov, P.; Coey, J.M.D.; Stampe, P.A.; Kennedy, R.J.; Moreira, E.C.; Sias, U.S. *Phys. Rev. B* **2006**, 74, 115307.
8. Fitzgerald, C.B.; Venkatesan, M.; Douvalis, A.P.; Huber, S.; Coey, J.M.D. *J. Appl. Phys.* **2004**, 95, 7390.
9. Punnoose, A.; Hays, J.; Thurber, A.; Engelhard, M.H.; Kukkadapu, R.K.; Wang, C. *Phys. Rev. B* **2005**, 72, 054402.
10. Adhikari, R.; Das, A.K.; Karmakar, D.; Rao, T.V.C.; Ghatak. *J. Phys. Rev. B* **2008**, 78, 024404.
11. Ogawa, H.; Nishikawa, M.; Abe, A. *J Appl Phys* **1982**, 53, 4448.
12. Fu, C.; Wang, J.; Yang, M.; Su, X.; Xu, J.; Jiang, B. *J Non-Crystalline Solids* **2011**, 357, 1172.
13. Kaur, J.; Kotnala, R.K.; Gupta, V.; Verma, K.C. *Indian J. of Pure and Appl. Phys.* 2012, 50, 57.

Advanced Materials Letters

Publish your article in this journal

[ADVANCED MATERIALS Letters](#) is an international journal published quarterly. The journal is intended to provide top-quality peer-reviewed research papers in the fascinating field of materials science particularly in the area of structure, synthesis and processing, characterization, advanced-state properties, and applications of materials. All articles are indexed on various databases including [DOAJ](#) and are available for download for free. The manuscript management system is completely electronic and has fast and fair peer-review process. The journal includes review articles, research articles, notes, letter to editor and short communications.

